Optical absorption spectra of doped and codoped Si nanocrystallites

L. E. Ramos,[1] Elena Degoli,[2] G. Cantele,[3] Stefano Ossicini,[2] D. Ninno,[3] J. Furthmüller,[1] and F. Bechstedt[1]
[1]*Institut für Festkörpertheorie und-optik, European Theoretical Spectroscopy Facility (ETSF), Friedrich-Schiller-Universität Jena, Max-Wien-Platz 1, D-07743 Jena, Germany*
[2]*Dipartimento di Scienze e Metodi dell'Ingegneria and CNR-INFM-S3, Università di Modena e Reggio Emilia, via Amendola 2, Padiglione Morselli, I-42100 Reggio Emilia, Italy*
[3]*Dipartimento di Scienze Fisiche, Coherentia CNR-INFM and Università di Napoli "Federico II", Complesso Universitario Monte S. Angelo, Via Cintia, I-80126 Napoli, Italy*
(Received 17 April 2007; revised manuscript received 19 November 2007; published 18 December 2008)

The effects of the incorporation of group-III (B and Al), group-IV (C and Ge), and group-V (N and P) impurities on the formation energies, electronic density of states, optical absorption spectra, and radiative lifetimes of Si nanocrystallites of different shape and with diameters up to 2 nm are studied by means of an *ab initio* pseudopotential method that takes into account spin polarization. The single doping with group-III or group-V impurities leads to significant changes on the onsets of the absorption spectra that are related to the minority-spin states. In contrast to the optical absorption spectra, the radiative lifetimes are sensitively influenced by the shape of the nanocrystallites, though this influence tends to disappear as the size of the nanocrystallites increase. Codoping is investigated for pairs of group-III and group-V impurities. We show that the impurity formation energies decrease significantly when the nanocrystallites are codoped with B and P or with Al and P. Additional peaks are introduced in the absorption spectra due to codoping, giving rise to a redshift of the absorption onset with respect to the undoped nanocrystallites. Those additional peaks are more intense when codoping is performed with two different species either of the group III or of the group V. The values of radiative lifetimes for the codoped nanocrystallites are mostly in between the values for the nanocrystallites doped with the impurities separately.

DOI: 10.1103/PhysRevB.78.235310 PACS number(s): 61.72.uf, 73.20.Hb, 73.22.−f, 78.67.−n

I. INTRODUCTION

Silicon nanocrystallites (NCs) and similar nanostructures have been intensively investigated in the last years due to their interesting quantum confinement properties.[1–3] The strong spatial localization of electrons and holes in Si NCs can enhance radiative recombination rates and give rise to luminescence. Among other known applications, research on Si NCs could lead to optoelectronic devices compatible with the consolidated Si technology. Optical gain in Si NCs has been reported,[4,5] and new devices have recently been suggested.[6,7]

The influence of the NC size on its optical properties is well known and confirmed by measurements.[8,9] As for molecules, NCs exhibit discrete energy spectra and the energetic separation between the lowest unoccupied molecular orbital (LUMO) and the highest occupied molecular orbital (HOMO) is controlled primarily by the size of the particle. Besides the NC size, the passivation of the dangling bonds and surface treatment of the nanocrystallite is known to be important for the electronic and optical properties.[9,10] For instance, the treatment of Si NCs with solutions containing Cl and F (Refs. 11–13) as well as oxidation[14,15] can alter significantly their luminescence properties. The shape of the NCs can be important for luminescence efficiency, since the changes in their internal electric fields can separate electrons and holes.[16] Less clear is the influence of doping on the luminescence properties observed in porous Si composed by Si NCs of different sizes. Besides being a fundamental process in semiconductor technology, doping of Si NCs is one of the several attempts to increase the photoluminescence (PL) intensity and to obtain optical gain.[4] Other Si nanostructures such as nanowires can be doped *n* type or *p* type and may become new building blocks of bipolar transistors and other electronic devices.[17] As for bulk Si, the doping of Si NCs may introduce additional levels close to the HOMO or LUMO, which are detected by available experimental techniques[18] and change the strength of the low-energy optical transitions.[19] Previous investigations on doping of porous Si doped with P show that the absorption in the infrared region of the spectrum is enhanced.[20,21] On the other hand quantum confinement is known to alter the electrical conductivity and concentration of carriers in Si NCs.[22] The heavy doping of silicon NCs with B and B-P codoping have been investigated recently as well as the effects of doping on the PL peaks and crystal growth.[23–27] In particular, it has been showed that a boron-phosphorus codoped Si NC always has an higher PL intensity than that of both a single (B or P) doped and of an undoped nanocrystallite.[25,27,28]

Apart from B and P doping of Si NCs, the effect of doping with group-IV species and other group-III and group-V species has not been investigated experimentally. To our knowledge, only one experiment on the role of N in the formation of Si NCs is reported in the literature.[29] On the other hand, *ab initio* theoretical investigations on doping of Si NCs comprehend many impurities, being carried out for Al (Refs. 30 and 31) and P,[30–34] and other group-III and group-V species in Si NCs. However, the investigations have been either restricted to small NCs or have not accounted for their optical properties.[33,35–37]

The optical absorption spectra and the effects of size and shape of doped Si NCs have not been studied so far. The knowledge of optical spectra of Si NCs and their dependence

on the size and shape could give an insight for the mechanisms of radiative recombination in doped NCs. In the following, we present an investigation of doped Si NCs, concerning their optical absorption properties as well as the influence of the shape and size on the incorporation of impurities. In addition to doping we study the effect of codoping with group-III and group-V impurities on the optical and electronic properties of Si NCs, as well as with the codoping with two different species either of the group III or group V.

To our knowledge the codoping with different impurities of the same group of the periodic table as well as other combinations of codoping with impurities of the group III and group V has not been investigated yet. In Sec. II we describe the computational methods and approaches applied. The results are discussed in Sec. III, and in Sec. IV we present a summary and conclusions. Our results are intended to serve as guide to interpret measurements in Si nanocrystallites, where group-III, group-IV, and group-V impurities are intentionally present or not.

II. METHODS

The density-functional theory (DFT) and generalized-gradient approximation (GGA),[38] as implemented in the Vienna *ab initio* simulation package, are employed to calculate the Kohn-Sham (KS) eigenvalues and total energies.[39,40] The interaction between valence electrons and atomic nuclei is modeled by pseudopotentials that correspond here to the so-called projector-augmented-wave data sets.[41] The pseudopotentials require a low-energy cutoff for plane waves in comparison with norm-conserving pseudopotentials and are suitable for the calculation of optical-matrix elements. An energy cutoff of 16 Ry suffices to achieve convergence of the interatomic forces. If the doping leads to a system with an odd number of electrons, we perform spin-polarized calculations. The Si NCs are modeled by using the supercell method and by means of simple-cubic supercells whose sizes vary according to the diameter of the NC. More than 15 Å of vacuum separate points localized at the surface of the NC and its images in the supercell method. The large size of the supercells justifies the restriction of the **k**-point sampling in the Brillouin zone to the Γ point. Dangling bonds at the surface of the Si NCs are passivated with H atoms, which excludes the possible effects of surface states and surface reconstructions from our investigation. Previous investigations on the localization of states near the HOMO and LUMO show that these states are not related to the H atoms at the surface of the nanocrystallites.[42] Therefore, the changes in the HOMO-LUMO gap of the Si NCs refer to quantum confinement effects and to the levels that may be introduced by the substitutional impurities considered.

We consider both spherical-like and faceted Si NCs. The spherical-like NCs are obtained by cutting Si atoms outside a sphere from bulk Si,[43] whereas the faceted NCs are resulting from a shell-by-shell construction procedure, in which one starts from a central atom and adds shells of atoms successively.[44–47] In Fig. 1 the spherical-like Si NCs are the clusters $Si_{29}H_{36}$, $Si_{87}H_{76}$, $Si_{147}H_{100}$, and $Si_{293}H_{172}$ and the faceted Si NCs are the clusters Si_5H_{12}, $Si_{17}H_{36}$, $Si_{41}H_{60}$, and $Si_{147}H_{148}$. Due to its small size the Si_5H_{12} NC could be classified either as spherical-like or faceted. The atomic sites of the Si NCs at their initial configuration resemble locally those of the diamond structure, where the atoms have a tetrahedral coordination. In both spherical-like and faceted Si NCs there is a Si atom at the center. The relaxation of the atomic positions in Si NCs is performed without any symmetry constraint in order to minimize the total energies and interatomic forces down to 20 meV/Å. The average radius of the Si NC is considered as the average distance of the H atoms with respect to the center of the Si NC. The substitutional impurity is localized at the center of the NC and is investigated in its neutral (groups III, IV, and V) and ionized states (groups III and V).[47] By considering only one impurity in the Si NCs we study a wide range of doping concentrations, which vary approximately from 2×10^{20} cm^{-3} (1 mol %) to 7×10^{21} cm^{-3} (20 mol %).

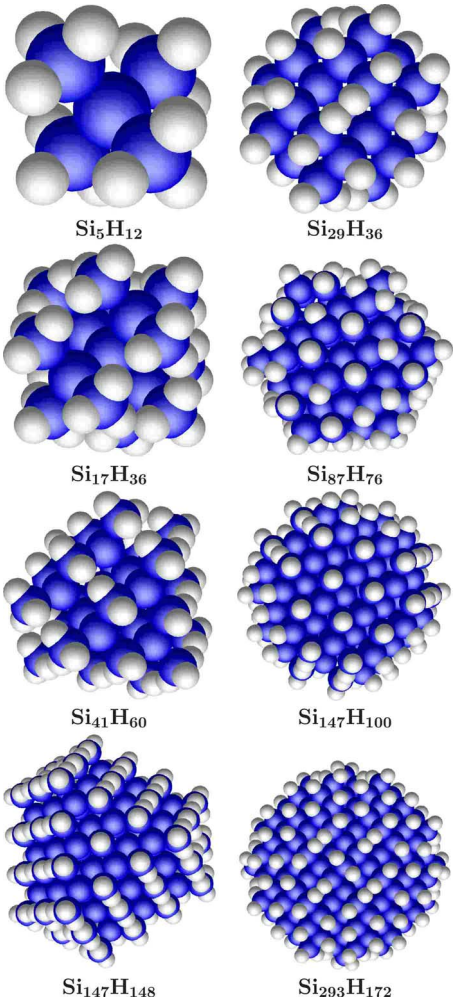

FIG. 1. (Color online) Faceted (left panels) and spherical-like (right panels) undoped Si NCs. The dark spheres represent the Si atoms and the light spheres represent the H atoms.

The codoping is studied for the $Si_{41}H_{60}$ and $Si_{147}H_{148}$ NCs, which contain facets, and the $Si_{87}H_{76}$ and $Si_{147}H_{100}$ NCs which have a spherical-like shape. Two Si atomic sites close to the center of the NC and in opposite directions are chosen as impurity sites. To evaluate effects of the energetic

stability of the impurity incorporation in the Si NC, we consider the case of double doping with group-III and group-V impurities in addition to codoping and single doping. Although the atomic sites near the center of the Si NC may not be the most energetically stable sites for all the impurities,[32,33,37] this choice evaluates the effects of an actual incorporation of impurities in the Si NC and allows a systematic comparison between all the considered systems. Chan *et al.*[34] reported that the most favorable site for the incorporation of the P impurity in Si NCS depends on the size of the NC. After a critical NC size the impurity may be incorporated either near the surface or at the center of the NC. For small NCs there is a tendency to the P impurity to be expelled to the surface.[34]

The formation energies of the doped Si NCs are calculated by means of a difference of total energies $E_{\mathrm{tot}}^{\mathrm{NC}:XY}$ $(X,Y=\mathrm{B},\mathrm{Al},\mathrm{N},\mathrm{P})$ and $E_{\mathrm{tot}}^{\mathrm{NC}}$, respectively, of the codoped (doped) and undoped Si NC, and estimates of the chemical potentials μ by

$$\Omega_f = E_{\mathrm{tot}}^{\mathrm{NC}:XY} - E_{\mathrm{tot}}^{\mathrm{NC}} + N_{\mathrm{Si}}\mu_{\mathrm{Si}} - N_X\mu_X - N_Y\mu_Y, \qquad (1)$$

where N_{Si} is the number of Si atoms removed from the Si NC, and N_X and N_Y are the number of the atomic species incorporated at substitutional sites in the NC. Estimates of the chemical potentials μ of the atomic-species reservoirs are obtained by means of the molecules and crystalline phases in which the atomic species occur in nature.[47] The chemical potential of the N reservoir is taken as the cohesive energy of the N_2 molecule divided by two $\mu_{\mathrm{N}}=-8.12$ eV. Estimates of chemical potentials of C, Si, and Ge are obtained from their diamond structure leading to $\mu_{\mathrm{C}}=-8.90$ eV, $\mu_{\mathrm{Si}}=-5.41$ eV, and $\mu_{\mathrm{Ge}}=-4.52$ eV, respectively. For Al the estimate of $\mu_{\mathrm{Al}}=-3.67$ eV was calculated for the face-centered cubic structure of this material. The chemical potential $\mu_{\mathrm{B}}=-6.40$ eV for the B reservoir is obtained from one of the most common structures for B known as T-50 (space group $P4_2/nnm$). We suppose a reservoir of black phosphorus to make an estimate of the chemical potential of the phosphorus reservoir $\mu_{\mathrm{P}}=-5.29$ eV.

The optical absorption spectra are calculated within the framework of the independent-particle approximation as the imaginary part of the complex dielectric function $\epsilon_{\mathrm{SC}}(\omega)$ corresponding to the supercell.[48] Since the absorption spectrum usually corresponds to the entire supercell (ϵ_{SC}) rather than to the NC (ϵ_{NC}), we extract ϵ_{NC} by applying a simple effective-medium theory $\epsilon_{\mathrm{SC}}(\omega)=f\epsilon_{\mathrm{NC}}(\omega)+(1-f)$, where f is the NC-supercell volume ratio.[45,46,49] A Lorentzian broadening of 50 meV is applied to all spectra. For undoped NCs and systems with discrete levels such as molecules, experimental curves of absorption, and emission spectra are usually very similar at their onsets and are shifted by the Stokes shift. Based on the optical matrix elements and on the assumption that the thermalization of electrons and holes is more efficient than the radiative recombination, we calculate the radiative lifetimes by $\tau=\Sigma_{ij}\exp[-\varepsilon_{ij}/k_BT]/\Sigma_{ij}W_{ij}\exp[-\varepsilon_{ij}/k_BT]$, where ε_{ij} are the transition energies, T is the absolute temperature, k_B is the Boltzmann constant, and W_{ij} are the radiative recombination rates, which are proportional to the refractive index n of the medium.[50] In the following the radiative lifetimes are discussed for $n=1.0$.

It is well known that the independent-particle approach severely underestimates the band-gap energy and that this inadequacy can be resolved through the inclusion of many-body corrections perturbatively, considering the self-energy corrections[51] by means of the GW method (Green's function and screened Coulomb potential) and the excitonic effects through the solutions of the Bethe-Salpeter equation (BSE) for the polarization function.[52] Nevertheless the results obtained within the independent-particle approach are interesting for the following reasons. First, the GW-BSE calculations are very computationally demanding, thus they can be used actually only for the small nanocrystallites[53] and surely not yet for unit cells containing hundreds of atoms. Second, the usual GW-BSE formalism must be extended to treat open-shell systems, i.e., systems with an odd number of electrons. Third, as recently showed in the case of doped[53] and undoped[54] nanocrystallites and nanowires[55] one observes an almost complete compensation of self-energy and excitonic effects, thus the GW-BSE band-gap values and optical features resemble the independent-particle ones in many aspects. This compensation for zero-dimensional nanomaterials was predicted theoretically by Delerue *et al.*[56] and by Porter *et al.*[57] Finally the trends observed in the optical properties for a huge number of systems regarding the dependence on nanocrystallite size, type, and number of dopants will remain similar on going from the independent-particle to the many-particle spectra. In the case of single doping the effects of spin polarization on the spectrum should be taken into account, what may make models within GW-BSE or even time-dependent DFT (Refs. 58 and 59) (TDDFT) too time consuming computationally in comparison with DFT.

In the case of doping with group-III and group-V neutral impurities, the spin polarization is taken into account within DFT-GGA, which implies two groups of electronic states associated with the spin up and spin down. Due to the presence of the impurity, the Si NC may have an odd number of electrons and one of the spin state groups has an extra electron. The model to calculate the dielectric function used previously for undoped nanocrystallites[42,44–46] had to be extended to account for the optical transitions of each spin component separately because there are unpaired electrons in the group-III and group-V doped Si NCs. In the model we consider that the electron does not change its spin during an optical transition. The final absorption spectrum results from the spin-up and spin-down contributions, though the lowest transition energy for each spin component can vary significantly. In the case of group-III (group-V) doping the lowest transition energy of the minority-spin (majority-spin) component is much smaller than the lowest energy of the majority-spin (minority-spin) component, due to the acceptor (donor) level in the gap.

III. RESULTS

A. Impurity formation energies

The impurity formation energies calculated by Eq. (1) are shown in Fig. 2 for the $Si_{41}H_{60}$, $Si_{87}H_{76}$, $Si_{147}H_{100}$, and $Si_{147}H_{148}$ NCs in the cases of single doping, codoping, and

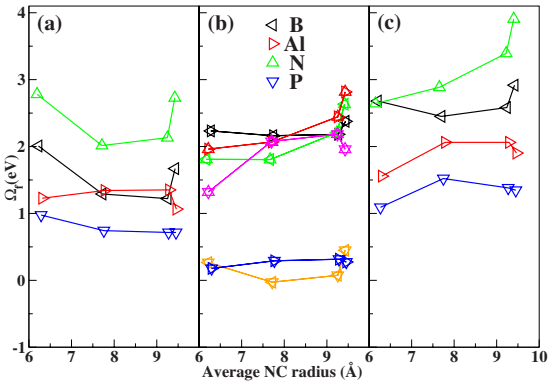

FIG. 2. (Color online) Impurity formation energies Ω_f for the Si NCs doped with a (a) single atom, (b) codoped, and (c) doped with two atoms of the same atomic species. We consider B (left triangle), Al (right triangle), N (up triangle), and P (down triangle). The overlap of triangles with different orientation at the same point indicates the codoping with two different species.

double doping. As expected from the high energetic stability of the N_2 molecule, the formation energy of the Si NCs doped with a single N is the highest among the atom impurities considered, followed by the Si NC doped with B, Al, and P. There is an overall tendency to increase the values of Ω_f if the Si NC is doped with two atoms of the same atomic species as shown in Figs. 2(a) and 2(c). The shape of the Si NC has an influence on the formation energy since the differences between the impurity formation energies of the $Si_{147}H_{100}$ and $Si_{147}H_{148}$ NCs may differ by about 0.5 eV. B-Al, Al-N, B-N, and N-P codoping lead to the highest impurity formation energies among the codoped Si NCs considered with energy values varying between 1 and 3 eV. The advantage of the codoping in comparison with single doping from the energetic point of view is clear in the case of B-P and Al-P codoping, where the formation energies calculated are lower than the single doping with B, P, and Al. Moreover, the values of impurity formation energies of the P- and Al-doped Si NCs are very similar in large and small NCs. An excess of P during the B-P and Al-P codoping favors the incorporation of the two impurities in Si NCs. Since the formation energy of the B double doping is higher than the P double doping, an excess of P during the doping may favor energetically the B-P codoping of Si NCs. An excess of P may also favor the codoping with Al and P as well.

B. Doping with group-III impurities

As shown in Fig. 3 the doping with group-III impurities has a strong influence on the optical absorption spectra of small Si NCs. Al-related absorption peaks can be about ten or twenty times more intense than the B-related absorption peaks, as shown in the panels for Si_4AlH_{12} and $Si_{16}AlH_{36}$ in Fig. 3. On the other hand the Al-related peaks become less intense much faster than the B-related peaks, as the size of the Si NC increases. The lowest transition energy of the neutral impurity tends to zero, as the size of the doped Si NC increases, because the energy difference between the HOMO and the LUMO of the minority-spin states tends to decrease

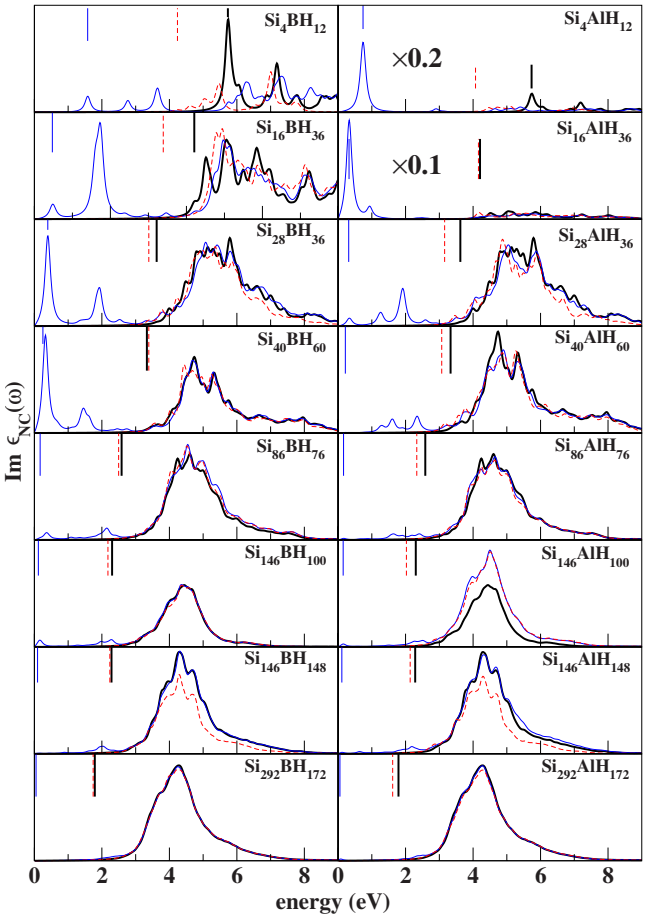

FIG. 3. (Color online) Optical absorption spectra (curves) and energetic position of the lowest optical transition (vertical lines from the top) for the undoped Si NCs (thick solid lines) and for Si NCs doped with group-III impurities in their neutral (thin solid line) and ionized (dashed lines) charge state. Unless a multiplication factor is indicated, the scale of Im $\epsilon_{NC}(\omega)$ axis is the same for each row of panels.

as the number of electronic states increases.[47] However, the oscillator strength of this transition tends to decrease for large doped Si NCs. The values of the lowest transition energies of the Si NCs doped with the ionized group-III impurities approach the lowest transition energy of the undoped Si NCs. For the largest doped Si NC the absorption spectrum looks practically the same as for the undoped Si NCs. This shows that changes in the spectra should be caused by neutral impurities.

Measurements of Chen and Shen[24] support a low influence of the B doping on the HOMO-LUMO gaps of Si NCs with average diameter of 5.1 nm. Even at high levels of doping with B, the measured values of the optical gap of Si NCs are a compromise between the gap of bulk Si and amorphous Si.[24] Fujii *et al.*[27] investigated B doping in Si NCs and observed higher PL intensity than the ones observed for undoped Si NCs. In qualitative agreement with the experiments, a tendency for increasing oscillator strengths near the absorption onset is visible for most of the calculated spectra of B-doped and Al-doped Si NCs in Fig. 3.[25]

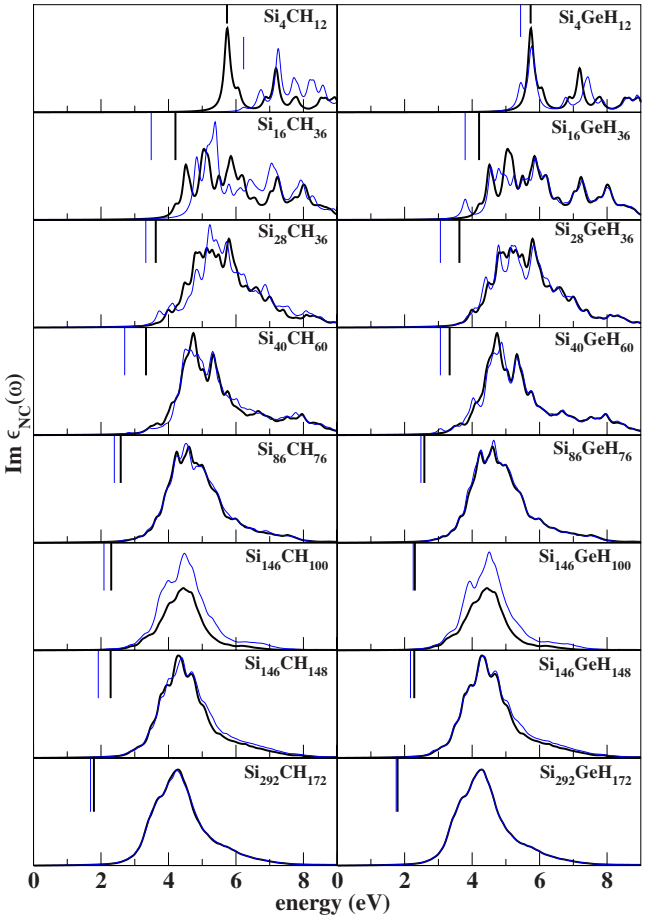

FIG. 4. (Color online) Optical absorption spectra (curves) and energetic position of the lowest optical transition (vertical lines from the top) for the undoped Si NCs (thick solid lines) and Si NCs doped with neutral (thin solid lines) group-IV impurities.

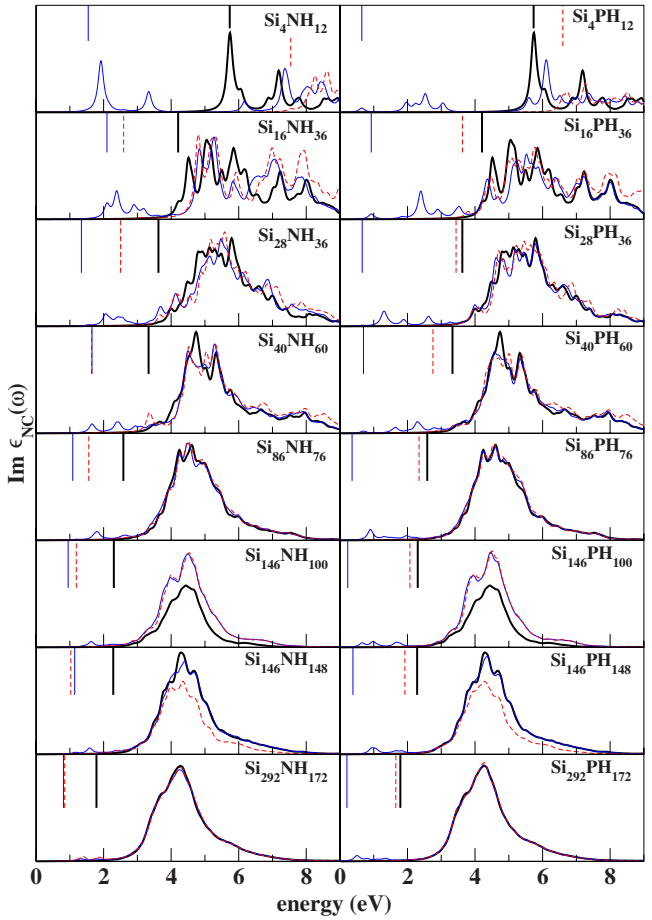

FIG. 5. (Color online) Optical absorption spectra (curves) and energetic position of the lowest optical transition (vertical lines from the top) for undoped Si NCs (thick solid lines) and for Si NCs doped with neutral (thin solid lines) and ionized (dashed lines) group-V impurities.

C. Doping with group-IV impurities

Since Ge is chemically similar to Si its incorporation at one Si site in the NCs should have little influence on the optical properties. In contrast to this, interesting properties arise when several Ge atoms are incorporated either at the center or at the surface of Si NCs.[42]

The absorption spectra of Si NCs doped with group-IV impurities in Fig. 4 show less and less influence of the doping as the size of the NCs increase. Although C is much smaller than Si and can displace significantly its neighboring Si atoms, the effect of its incorporation on the spectra is similar to that of the Ge incorporation. The lowest transition energies of Si NCs doped with group-IV impurities are in general lower than the corresponding transitions for the undoped Si NCs. Since the Si-C bond length is shorter than the Si-Si bond length, the size of the Si_4CH_{12} NC is quite reduced, and consequently the lowest transition energy is higher than for the undoped Si_5H_{12} NC. Apart from the variations in the spectra for small Si NCs, there is no apparent correlation between the shape of the NC and the features of the absorption spectra.

D. Doping with group-V impurities

The deep-donor and shallow-donor characters, respectively, of the neutral N and P impurities change significantly the optical absorption spectra of doped Si NCs, as shown in Fig. 5. On the other hand the impurity-related peaks in the absorption are not so intense as in the case of the Si NCs doped with group-III impurities. Since N on the substitutional site gives rise to a deep donor, the lowest transition energies for the N-doped Si NCs are the highest among the group-III and P-doped Si NCs considered. Moreover, the energetic position of the N impurity level allows the lowest energy transition energies of the ionized and neutral N-doped Si NC to be nearly equal in some cases. It is interesting to note that the PL spectra of Si NCs obtained from thermally induced nucleation in amorphous Si-rich nitride films show features in the 1.0–1.5 eV region, thus in the region where we observe the N impurity-level localization.[60] On the other hand, the values of the lowest transition energies of P-doped Si NCs are similar to those of B-doped and Al-doped Si NCs. The values of the lowest transition energies of the Si NCs doped with an ionized P are larger than the lowest transition energy of the Si NC doped with a neutral P impurity. Except

for the small NCs Si_4NH_{12} and Si_4PH_{12}, the spectra of the Si NCs doped with ionized group-V impurities resemble the ones of undoped Si NCs. Since the donor impurity levels of P are shallower than the ones for N, the lowest transition energy of Si NC doped with the ionized P impurity is closer to the energy of the HOMO-LUMO gap of the undoped Si NC.

The impurity-related peaks of the absorption spectra for the neutral P impurity are consistent with the experimental observation of P doping in Si NCs.[27,28] In some doped samples the absorption occurs in the infrared region, which corresponds to the energy range of the peaks shown in Fig. 5.[21] In qualitative agreement with our theoretical predictions, the impurity-related levels are found to depend on the size of large Si NCs (80–200 nm) doped with P.[18] We also obtain a qualitative agreement with the measurements made by Fujii *et al.*[25] for Si NCs doped with either B or P. As depicted from our calculations for the absorption spectra in Fig. 5 and from the measurements reported in Ref. 25, the enhancement in the absorption and emission can only be attributed to either B doping or P doping in small Si NCs. For large Si NCs the role of P doping is predicted to be more important since the B-related peaks in Fig. 3 practically vanish for the largest Si NC, in contrast to the P-related peaks in Fig. 5.

E. Effects of spin polarization on the spectra

In order to study the influence of spin polarization on the absorption spectra of group-III and group-V Si NCs, we considered separately spin-up and spin-down electronic states in the calculation of the macroscopic dielectric function. The role played by spin polarization on the spectra of doped Si NCs is shown in Figs. 3 and 5. Since the number of electrons in the two groups of spin states differs by one, the HOMO and LUMO of each group of states differ in energy. The minority-spin group of states has one electron less and its HOMO and LUMO are very close in energy, whereas the HOMO-LUMO energy difference of the majority-spin states corresponds roughly to the energy difference between the defect level and the LUMO of the undoped system. In Fig. 6, we show the contributions for the optical spectrum of the majority-spin states and of the minority-spin states separately for the $Si_{87}H_{76}$ NC doped with B, Al, N, and P neutral impurities. The HOMO-LUMO transition of the minority-spin states presents a very high oscillator strength, and the transitions involving the impurity state and states below the HOMO give rise to intense peaks in the absorption. On the other hand, the spectra corresponding to the majority-spin states are very similar to the one of the undoped Si NCs in Fig. 6, apart from the height which should be nearly one-half of the undoped Si NCs.

F. Codoping with group-III and group-V impurities

In Figs. 7–10 we present the density of states (DOS) and optical absorption spectra of Si NCs codoped with group-III and group-V impurities in comparison with the density of states and spectra of undoped Si NCs. Since the DOS of the undoped and codoped Si NCs correspond to different systems a common energy reference had to be determined for

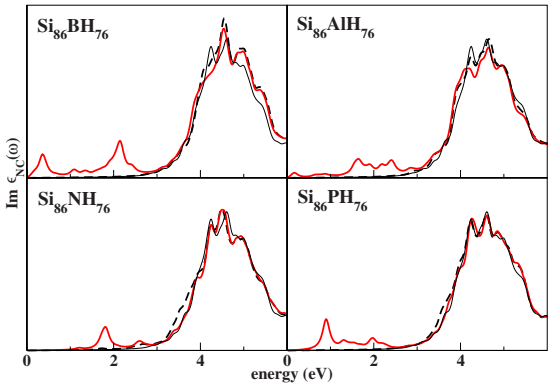

FIG. 6. (Color online) Partial contributions for the optical absorption spectra from the minority-spin states (thick solid line) and from the majority-spin states (dashed line) for four doped Si NCs, in comparison with the absorption spectrum of the undoped $Si_{87}H_{76}$ NC (thin solid line). The intensity of the absorption spectrum of the undoped NC was divided by 2 for better comparison with the other curves.

the two systems. We use average values of the electrostatic potential at the vacuum region of the two systems to align the energies of the two systems.[61] Doping of Si NCs with a single B impurity leads to a shallow acceptor level, whereas doping with a single N impurity leads to a deep donor level. The B and N impurity levels are present when the Si NC is doped with both impurities simultaneously as can be seen in Fig. 7. Apart from the states near the HOMO and LUMO, the DOSs of Si NCs codoped with B and N keep most of their features at other energy ranges, especially for large Si NCs. The impurity state which originated from the B impurity is filled with two electrons and coincides with the HOMO of the codoped Si NC. The energetic position of the lowest transition energy is about one-half the undoped Si NC since the N impurity level is located close the mid gap.

As shown in Fig. 8, codoping with Al and N leads to similar DOS and optical absorption spectra as in the case of

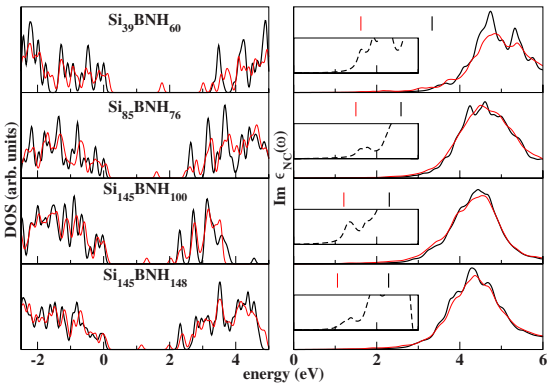

FIG. 7. (Color online) Electronic density of states (left panels) and optical absorption spectra (right panels) for B-N codoped Si NCs (thin solid lines) in comparison with those of the undoped Si NCs (thick solid lines). The vertical lines indicate the position of the lowest transition energy. In the right panels, the insets show the difference of absorption intensities between the codoped and undoped cases (dashed lines), enlarged by a factor 100.

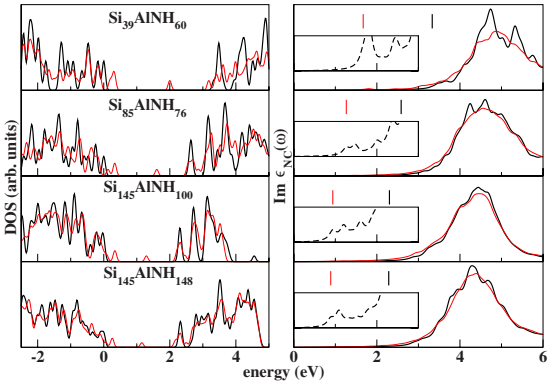

FIG. 8. (Color online) Electronic density of states (left panels) and optical absorption spectra (right panels) for Al-N codoped Si NCs (thin solid lines) in comparison with those of the undoped Si NCs (thick solid lines). The vertical lines indicate the position of the lowest transition energy. In the right panels, the insets show the difference of absorption intensities between the codoped and undoped cases (dashed lines), enlarged by a factor 100.

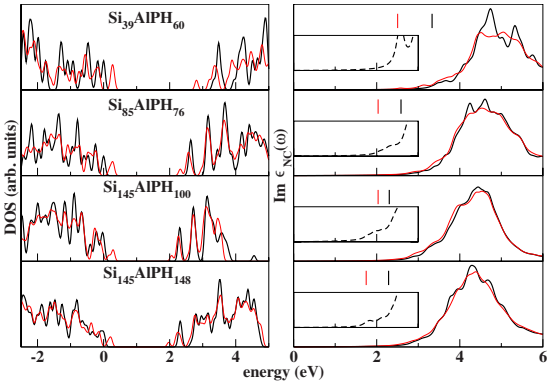

FIG. 10. (Color online) Electronic density of states (left panels) and optical absorption spectra (right panels) for Al-P codoped Si NCs (thin solid lines) in comparison with those of the undoped Si NCs (thick solid lines). The vertical lines indicate the position of the lowest transition energy. In the right panels, the insets show the difference of absorption intensities between the codoped and undoped cases (dashed lines), enlarged by a factor 100.

codoping with B and N. The impurity level associated with Al contains two electrons and is deeper than the one associated with B, which leads to even lower lowest transition energy than in the case of codoping with B and N. Codoping with B and P impurities introduces a B-related level and P-related level, as shown in DOS in Fig. 9. The B-related and P-related levels are the HOMO and the LUMO of the codoped Si NC, respectively. Since both levels are shallow in comparison with the HOMO and the LUMO of the undoped Si NC, the lowest transition energies are slightly redshifted in energy in comparison with the lowest transition energy of the undoped Si NCs. Indeed, a redshift of the PL luminescence peak is observed in experiments involving the B-P codoping.[27] Although the Al-related levels in Fig. 10 are deeper than the B-related levels in Fig. 9, the lowest transition energies in the case of Al-P codoping are similar to the ones corresponding to B-P codoping. A comparison of the

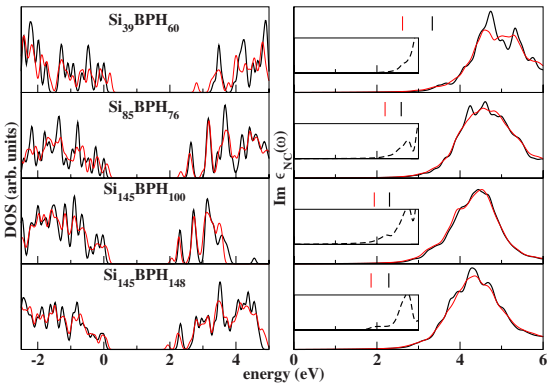

FIG. 9. (Color online) Electronic density of states (left panels) and optical absorption spectra (right panels) for B-P codoped Si NCs (thin solid lines) in comparison with those of the undoped Si NCs (thick solid lines). The vertical lines indicate the position of the lowest transition energy. In the right panels, the insets show the difference of absorption intensities between the codoped and undoped cases (dashed lines), enlarged by a factor 100.

spectra of B-N, Al-N, B-P, and Al-P codoped Si NCs with the ones of the undoped Si NCs, apparently shows that codoping with group-III and group-V impurities do not introduce any feature in the optical absorption spectra. The fact that the lowest transition energies of Si NCs codoped with group III and P are closer to the lowest transition energies of the undoped Si NCs can be seen as an advantage in comparison with codoping with group III and N for instance. Low-intensity absorption peaks (see insets of Figs. 7–10), which correspond to the transitions from the group-III-related states and states below to the group-V-related state and states above, appear near the onset of the absorption. Those peaks show that transitions involving the group-V-related impurity level are not forbidden, though they have low oscillator strengths. Our results for the absorption suggest that a significant increase in PL intensities observed in experiments[27,28] cannot be attributed to codoping Si NCs. While the absorption and emission spectra of undoped Si NCs may resemble each other, the emission of codoped Si NCs may differ significantly from the absorption since the codoping is intended to prevent processes such as nonradiative Auger recombination. Therefore, the apparent disagreement with the experimental observation can be explained in terms of the theoretical model applied.

Concerning the influence of the size of the Si NCs, we notice that the DOS and the optical absorption spectra of the $Si_{41}H_{60}$ NC experience more changes due to the codoping. Although there are some changes in the DOS of the $Si_{147}H_{100}$ and $Si_{147}H_{148}$ NCs, the optical absorption spectra of the codoped and undoped Si NCs look very similar even at energies near the absorption onset. The values of the average radii of the $Si_{147}H_{100}$ and $Si_{147}H_{148}$ NCs differ by less than 0.3 Å both in the codoped and undoped cases. This indicates that influence of the size of the codoped Si NCs on the optical absorption spectra is higher than the influence of their shape.

G. Codoping with group-III impurities

The effects of the codoping with B and Al on the DOS and on the optical absorption spectra are shown in Fig. 11.

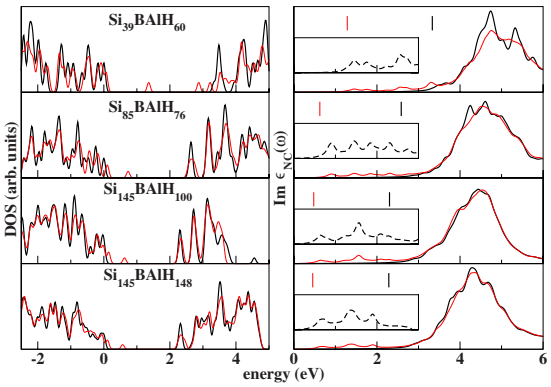

FIG. 11. (Color online) Electronic density of states (left panels) and optical absorption spectra (right panels) for B-Al codoped Si NCs (thin solid lines) in comparison with those of the undoped Si NCs (thick solid lines). The vertical lines indicate the position of the lowest transition energies. In the right panels, the insets show the difference of absorption intensities between the codoped and undoped cases (dashed lines), enlarged by a factor 10.

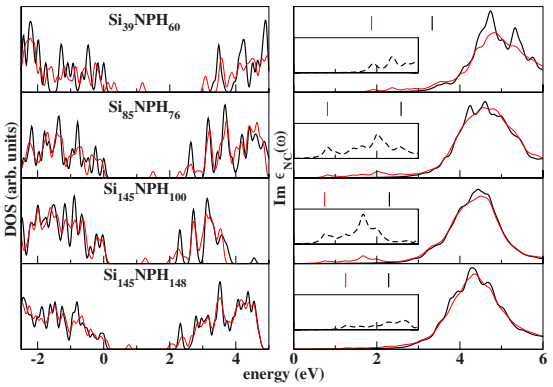

FIG. 12. (Color online) Electronic density of states (left panels) and optical absorption spectra (right panels) for N-P codoped Si NCs (thin solid lines) in comparison with those of the undoped Si NCs (thick solid lines). The vertical lines indicate the position of the lowest transition energies. In the right panels, the insets show the difference of absorption intensities between the codoped and undoped cases (dashed lines), enlarged by a factor 10.

Codoping with two group-III atomic species leads to two shallow levels related to the B and Al. Since the codoped Si NC has two electrons less than the undoped Si NC, the Al-related level is the LUMO and the B-related level is the HOMO of the electron system. As a result the lowest transition energies of the B-Al codoped Si NCs are low in comparison with the lowest transition energies of the undoped Si NCs. The DOS of the codoped Si NCs is not significantly changed for states below the HOMO and above the LUMO, as for the codoping with group-III and group-V impurities. In contrast with the codoping with group-III and group-V impurities the B-Al codoped Si NC shows peaks up to ten times more intense than the ones resulting from codoping with group-III and group-V impurities. Those peaks are related to optical transitions involving states below the HOMO and the Al-related impurity level, i.e., the LUMO of the B-Al codoped Si NC. There is no indication that those peaks would vanish for large Si NCs, which shows that the many transitions involving the Al-related level have high oscillator strengths. The energy range where the peaks occur and their absorption intensity may suggest applications of the B-Al codoped Si NCs in devices operating in the infrared and near-infrared radiation.

H. Codoping with group-V impurities

Codoping with the two group-V atomic species leads to a similar situation as the codoping with two group-III atomic species, in the sense that the N-related impurity level is the HOMO and the P-related impurity level is the LUMO of the codoped Si NC. As in the case of B-Al codoping, the lowest transition energies in Fig. 12 are considerably reduced with respect to the lowest transition energies of the undoped Si NCs. The DOS is mostly affected in the gap energy region as in the previous codoping cases considered. Peaks in the energy range of the infrared radiation are also present in the optical absorption spectra, and are related to the level introduced by the P impurity. The optical absorption spectrum for the $Si_{147}H_{148}$ NC suggests that the absorption peaks due to the codoping with N and P may disappear or be less intense for large Si NCs. As for codoping with group-III impurities, the peaks resulting from the codoping with group-V impurities may be up to ten times more intense than the peaks which appear due to the simultaneous codoping with group-III and group-V impurities.

I. Radiative lifetimes

The radiative lifetimes calculated at room temperature ($T=300$ K) and shown in Fig. 13 are sensitive to the size and the shape of doped and undoped Si NCs. Since the radiative lifetimes are calculated as an average over all the states, only few differences were observed between the radiative lifetimes of neutral and ionized group-III and group-V impurities. There is a general tendency of the radiative lifetimes of doped Si NCs to approach the value of the undoped Si NCs for large NCs. The radiative lifetimes of small faceted Si NCs doped with B, Al, N, and C can be 2–6 orders of magnitude larger than those of undoped Si NCs of equal size. In the case of doping with P, the differences between the radiative lifetimes of doped and undoped Si NCs are the smallest among the doped NCs considered. Since in the experiments the doped Si NCs have diameters typically larger than 2 nm,[18,21] the radiative lifetimes of doped Si NCs in Fig. 13 should not differ much from those of large undoped Si NCs.

A comparison between the radiative lifetimes of undoped, doped, and codoped Si NCs is shown in Fig. 14. An overall increase in the radiative lifetimes with increasing size of the Si NCs is predicted by our calculations. Our results indicate that the values of the radiative lifetimes may change by 1 order of magnitude due to the shape of the NC. For the largest Si NCs considered, there is a tendency to reduce the radiative lifetimes when the NC is doped or codoped. Although energetically unfavored, the codoping with N and P is the most effective combination to reduce the radiative life-

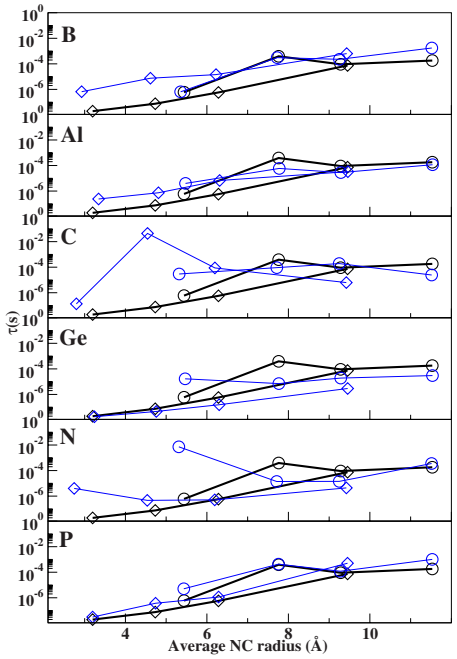

FIG. 13. (Color online) Radiative lifetimes of spherical-like (circles) and faceted (diamonds) Si NCs versus the average radius of the NC. The radiative lifetimes of Si NCs doped with neutral impurities (thin solid lines) are shown in comparison with those of undoped Si NCs (thick solid lines).

times of Si NCs in comparison with the undoped Si NCs. For B-Al, B-N, B-P, and Al-N codopings the values of radiative lifetimes for the codoped Si NCs are mostly in between the values for the Si NCs doped with each of the impurities separately. It is interesting to notice that the codoping with Al and P reduces the radiative lifetimes in comparison with the case of single doping with the same impurities, besides being favored energetically.

IV. SUMMARY AND CONCLUSIONS

By means of an *ab initio* pseudopotential method we studied the effects of size and shape on the optical absorption spectra, and radiative lifetimes of Si NCs doped with group-III, group-IV, and group-V impurities. Our calculations show that the doping with group-IV impurities reduces slightly the lowest transition energy of the Si NCs, though the effects of the doping on the spectra are not significant for large NCs. On the other hand, the doping with group-III and group-V impurities leads to several peaks at lower energies than the HOMO-LUMO gap of the undoped Si NCs. Those peaks are related to transitions involving minority-spin states. Except for N-doped Si NCs, the lowest transitions energies of doped Si NCs occur at lower energies than the ones of undoped Si NCs and the lowest transition energies of Si NCs doped with ionized impurities tend to approach the lowest transition energies of undoped Si NC, as the size of the NC increases. No feature in the absorption spectra suggests a dependence on the shape of the doped Si NCs. Our results for the spectra are in qualitative agreement with experiments where codoping with B and P in Si NCs is investigated. The radiative lifetimes calculated show a large range of variation for small NCs as well as small differences related to the shape of the doped Si NCs. However, the trend of the radiative lifetimes indicates that no dependence on the shape should be noticed for large doped Si NCs. Except for doping with Ge, an increase in the radiative lifetimes due to the doping occurs in the small Si NCs.

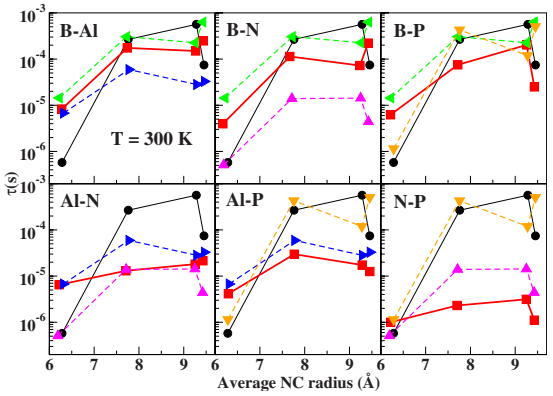

FIG. 14. (Color online) Radiative lifetimes versus radius of undoped (circles), codoped (squares), and doped Si NCs (dashed lines/triangles). The Si NCs doped with a single impurity are doped with B (left triangle), Al (right triangle), N (up triangle), and P (down triangle).

Our calculations indicate that codoping involving P atoms tends to lower the energy required to incorporate impurities. Codoping with Al and P and codoping with B and P are the combinations that lead to the lowest impurity formation energies. Codoping with group-III and group-V impurities leads to a redshift of the onset of the absorption spectra and results in low-intensity peaks related to transitions involving the HOMO and LUMO, which is in fair agreement with the experiments. On the other hand, codoping with two different group-III impurities and two different group-V impurities introduces more peaks in the absorption spectra, which are more intense and related to the transitions involving the impurity level that is unoccupied. In particular, the combination of B-Al codoping gives rise to intense optical transitions below the fundamental gap of the NC, which can alter the emission properties of the Si NCs significantly. We find an overall tendency of increasing of radiative lifetimes with increasing size of the Si NCs. In most cases and for large Si NCs, the values of the radiative lifetimes of codoped Si NCs are in between the values for single-doped Si NCs single doped. Codoping with Al and P and codoping with N-P are the most effective combination of impurities to reduce the radiative lifetimes. Since the codoping with Al and P is as favored energetically as the B-P codoping and reduces the radiative lifetimes, our results indicate that Al-P codoping can be of interest in the case of Si NCs.

ACKNOWLEDGMENTS

The authors would like to thank the European Commission in the NANOQUANTA network of excellence (Contract No. NMP4-CT-2004-500198) and the German Federal Min-

istry of Education and Research (BMFB) within the program "Basic research on renewable energy sources and efficient energy applications." The calculations were performed at the John von Neumann Institute for Computing (NIC) in Jülich, Germany (Grant No. HJN21). We acknowledge also the support of the MIUR PRIN (2005) Italy, of the CNR-CNISM "Progetto Innesco," and of the CRUI Vigoni Project (2005–2006) Italy-Germany.

[1] A. G. Cullis, L. T. Canham, and P. D. J. Calcott, J. Appl. Phys. **82**, 909 (1997).
[2] O. Bisi, S. Ossicini, and L. Pavesi, Surf. Sci. Rep. **38**, 1 (2000).
[3] S. Ossicini, L. Pavesi, and F. Priolo, *Light Emitting Silicon for Microphotonics, Springer Tracts in Modern Physics* (Springer, Berlin, 2003), Vol. 194.
[4] L. Pavesi, L. Dal Negro, C. Mazzoleni, G. Franzò, and F. Priolo, Nature (London) **408**, 440 (2000).
[5] L. Dal Negro, M. Cazzanelli, L. Pavesi, S. Ossicini, D. Pacifici, G. Franzò, and F. Priolo, Appl. Phys. Lett. **82**, 4636 (2003).
[6] J. Linnros, Nature Mater. **4**, 117 (2005).
[7] R. J. Walters, G. I. Bourianoff, and H. A. Atwater, Nature Mater. **4**, 143 (2005).
[8] S. Furukawa and T. Miyasato, Phys. Rev. B **38**, 5726 (1988).
[9] S. Schuppler, S. L. Friedman, M. A. Marcus, D. L. Adler, Y.-H. Xie, F. M. Ross, Y. J. Chabal, T. D. Harris, L. E. Brus, W. L. Brown, E. E. Chaban, P. F. Szajowski, S. B. Christman, and P. H. Citrin, Phys. Rev. B **52**, 4910 (1995).
[10] A. Puzder, A. J. Williamson, J. C. Grossman, and G. Galli, J. Chem. Phys. **117**, 6721 (2002).
[11] L. Seals, J. L. Gole, L. A. Tse, and P. J. Hesketh, J. Appl. Phys. **91**, 2519 (2002).
[12] J. L. Gole, J. A. DeVincentis, L. Seals, P. Lillihei, S. M. Prokes, and D. A. Dixon, Phys. Rev. B **61**, 5615 (2000).
[13] S. M. Prokes, W. E. Carlos, L. Seals, and J. L. Gole, Phys. Rev. B **62**, 1878 (2000).
[14] M. V. Wolkin, J. Jorne, P. M. Fauchet, G. Allan, and C. Delerue, Phys. Rev. Lett. **82**, 197 (1999).
[15] A. A. Seraphin, E. Werwa, and K. D. Kolenbrander, J. Mater. Res. **12**, 3386 (1997).
[16] A. M. Stoneham and B. A. McKinnon, J. Phys.: Condens. Matter **10**, 7665 (1998).
[17] Y. Cui and C. M. Lieber, Science **291**, 851 (2001).
[18] B. J. Pawlak, T. Gregorkiewicz, C. A. J. Ammerlaan, W. Takkenberg, F. D. Tichelaar, and P. F. A. Alkemade, Phys. Rev. B **64**, 115308 (2001).
[19] L. Burstein, Y. Shapira, J. Partee, J. Shinar, Y. Lubianiker, and I. Balberg, Phys. Rev. B **55**, R1930 (1997).
[20] M. Fujii, A. Mimura, S. Hayashi, Y. Yamamoto, and K. Murakami, Phys. Rev. Lett. **89**, 206805 (2002).
[21] A. Mimura, M. Fujii, S. Hayashi, D. Kovalev, and F. Koch, Phys. Rev. B **62**, 12625 (2000).
[22] V. Y. Timoshenko, T. Dittrich, V. Lysenko, M. G. Lisachenko, and F. Koch, Phys. Rev. B **64**, 085314 (2001).
[23] L. Boarino, F. Geobaldo, S. Borini, A. M. Rossi, P. Rivolo, M. Rocchia, E. Garrone, and G. Amato, Phys. Rev. B **64**, 205308 (2001).
[24] H. Chen and W. Z. Shen, J. Appl. Phys. **96**, 1024 (2004).
[25] M. Fujii, K. Toshikiyo, Y. Takase, Y. Yamaguchi, and S. Hayashi, J. Appl. Phys. **94**, 1990 (2003).
[26] W. Wensheng, W. Tianmin, Z. Chunxi, L. Guohua, H. Hexiang, and D. Kun, Vacuum **74**, 69 (2004).
[27] M. Fujii, Y. Yamaguchi, Y. Takase, K. Ninomiya, and S. Hayashi, Appl. Phys. Lett. **85**, 1158 (2004).
[28] M. Fujii, Y. Yamaguchi, Y. Takase, K. Ninomiya, and S. Hayashi, Appl. Phys. Lett. **87**, 211919 (2005).
[29] V. Mulloni, P. Bellutti, and L. Vanzetti, Surf. Sci. **585**, 137 (2005).
[30] Z. Zhou, R. A. Friesner, and L. Brus, J. Am. Chem. Soc. **125**, 15599 (2003).
[31] T. Blomquist and G. Kirczenow, Nano Lett. **4**, 2251 (2004).
[32] D. V. Melnikov and J. R. Chelikowsky, Phys. Rev. Lett. **92**, 046802 (2004).
[33] G. Cantele, E. Degoli, E. Luppi, R. Magri, D. Ninno, G. Iadonisi, and S. Ossicini, Phys. Rev. B **72**, 113303 (2005).
[34] T.-L. Chan, M. L. Tiago, E. Kaxiras, and J. R. Chelikowsky, Nano Lett. **8**, 596 (2008).
[35] C. Majumder and S. K. Kulshreshtha, Phys. Rev. B **70**, 245426 (2004).
[36] Z. Zhou, M. L. Steigerwald, R. A. Friesner, L. Brus, and M. S. Hybertsen, Phys. Rev. B **71**, 245308 (2005).
[37] S. Ossicini, E. Degoli, F. Iori, E. Luppi, R. Magri, G. Cantele, F. Trani, and D. Ninno, Appl. Phys. Lett. **87**, 173120 (2005).
[38] Y. Wang and J. P. Perdew, Phys. Rev. B **44**, 13298 (1991).
[39] G. Kresse and J. Furthmüller, Comput. Mater. Sci. **6**, 15 (1996).
[40] G. Kresse and J. Furthmüller, Phys. Rev. B **54**, 11169 (1996).
[41] G. Kresse and D. Joubert, Phys. Rev. B **59**, 1758 (1999).
[42] L. E. Ramos, J. Furthmüller, and F. Bechstedt, Phys. Rev. B **72**, 045351 (2005).
[43] E. Degoli, G. Cantele, E. Luppi, R. Magri, D. Ninno, O. Bisi, and S. Ossicini, Phys. Rev. B **69**, 155411 (2004).
[44] L. E. Ramos, J. Furthmüller, and F. Bechstedt, Phys. Rev. B **71**, 035328 (2005).
[45] L. E. Ramos, J. Furthmüller, and F. Bechstedt, Phys. Rev. B **70**, 033311 (2004).
[46] L. E. Ramos, J. Furthmüller, and F. Bechstedt, Appl. Phys. Lett. **87**, 143113 (2005).
[47] L. E. Ramos, E. Degoli, G. Cantele, S. Ossicini, D. Ninno, J. Furthmüller, and F. Bechstedt, J. Phys.: Condens. Matter **19**, 466211 (2007).
[48] B. Adolph, J. Furthmüller, and F. Bechstedt, Phys. Rev. B **63**, 125108 (2001).
[49] F. Sottile, F. Bruneval, A. G. Marinopoulos, L. K. Dash, S. Botti, V. Olevano, N. Vast, A. Rubio, and L. Reining, Int. J. Quantum Chem. **102**, 684 (2005).
[50] C. Delerue, G. Allan, and M. Lannoo, Phys. Rev. B **48**, 11024 (1993).
[51] L. Hedin, Phys. Rev. **139**, A796 (1965).
[52] G. Onida, L. Reining, and A. Rubio, Rev. Mod. Phys. **74**, 601 (2002) and references therein.
[53] S. Ossicini, E. Degoli, F. Iori, O. Pulci, G. Cantele, R. Magri, O. Bisi, F. Trani, and D. Ninno, Surf. Sci. **601**, 2724 (2007).

[54] E. Luppi, F. Iori, R. Magri, O. Pulci, S. Ossicini, E. Degoli, and V. Olevano, Phys. Rev. B **75**, 033303 (2007).
[55] M. Bruno, M. Palummo, A. Marini, R. Del Sole, V. Olevano, A. N. Kholod, and S. Ossicini, Phys. Rev. B **72**, 153310 (2005).
[56] C. Delerue, M. Lannoo, and G. Allan, Phys. Rev. Lett. **84**, 2457 (2000).
[57] A. R. Porter, M. D. Towler, and R. J. Needs, Phys. Rev. B **64**, 035320 (2001).
[58] I. Vasiliev, S. Öğüt, and J. R. Chelikowsky, Phys. Rev. B **65**, 115416 (2002).
[59] M. L. Tiago and J. R. Chelikowsky, Phys. Rev. B **73**, 205334 (2006).
[60] L. Dal Negro, J. H. Yi, J. Michel, L. C. Kimerling, S. Hamel, A. Williamson, and G. Galli, IEEE J. Sel. Top. Quantum Electron. **12**, 1628 (2006).
[61] S. Pöykkö, M. J. Puska, and R. M. Nieminen, Phys. Rev. B **53**, 3813 (1996).